Science of the Total Environment 666 (2019) 414–422

Contents lists available at ScienceDirect

Science of the Total Environment

journal homepage: www.elsevier.com/locate/scitotenv

Characterization of perfluoroalkyl substances in sediment cores from High and Low Arctic lakes in Canada

John J. MacInnis [a], Igor Lehnherr [b], Derek C.G. Muir [c], Roberto Quinlan [d], Amila O. De Silva [c,*]

[a] Department of Chemistry, Memorial University, St. John's, Newfoundland and Labrador A1B 3X7, Canada
[b] Department of Geography, University of Toronto, Mississauga, Ontario L5L 1C6, Canada
[c] Aquatic Contaminants Research Division, Environment and Climate Change Canada, Burlington, Ontario L7S 1A1, Canada
[d] Department of Biology, York University, Toronto, Ontario M3J 1P3, Canada

HIGHLIGHTS

- Increasing temporal trends were found for PFOA, PFDA, PFBS, and PFOS in Lake Hazen.
- Increasing temporal trends were found for PFHpA, PFOA, PFNA, and PFUnDA in Lake B35.
- Temporal trends demonstrate the continuous delivery of PFASs to the Canadian Arctic.
- Temporal trends follow historical market changes in PFAS manufacturing inventories.
- Faster deposition rates for PFASs in Lake Hazen may be due to enhanced glacier melt.

GRAPHICAL ABSTRACT

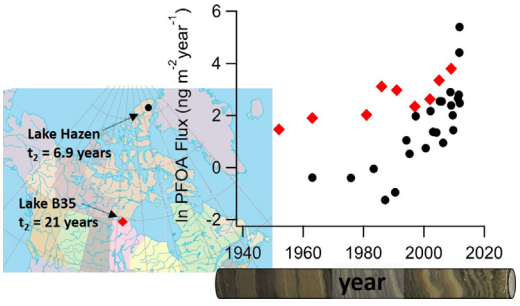

ARTICLE INFO

Article history:
Received 22 October 2018
Received in revised form 8 February 2019
Accepted 13 February 2019
Available online 15 February 2019

Editor: Adrian Covaci

Keywords:
Perfluoroalkyl substances (PFASs)
Temporal trends
Climate change
Glacier melt
Flux
Emissions

ABSTRACT

Perfluoroalkyl substances (PFASs) are synthetic environmentally-persistent pollutants that are amenable to long-range transport and accumulation in remote Arctic ecosystems. In this study, historical inventories of twenty-three PFASs (i.e. C_4-C_{14}, C_{16} perfluoroalkane carboxylic acids (PFCAs); C_4, C_6-C_8, C_{10} perfluoroalkane sulfonic acids (PFSAs); perfluoro-4-ethyl-cyclohexane sulfonic acid (PFECHS); dodecafluoro-3H-4,8-dioxanonanoic acid (ADONA); 8-chloro-perfluoro-1-octane sulfonic acid (8-Cl-PFOS); chlorinated polyfluorinated ether sulfonic acids (Cl-PFESAs) including 9-chlorohexadecafluoro-3-oxanonane-1-sulfonic acid (6:2 Cl-PFESA) and 11-chloroeicosafluoro-3-oxaundecane-1-sulfonic acid (8:2 Cl-PFESA); as well as perfluorooctane sulfonamide (FOSA)) are determined in two intact sediment cores collected from Lake Hazen, located in northern Ellesmere Island at 82° N in 2012 and Lake B35, located in central Nunavut at 64° N in 2009. In Lake Hazen, fluxes of perfluorooctanoic acid (PFOA), perfluorodecanoic acid (PFDA), perfluorobutane sulfonic acid (PFBS), and perfluorooctane sulfonic acid (PFOS) increased during 1963–2011. In Lake B35, fluxes of perfluoroheptanoic acid (PFHpA), PFOA, perfluorononanoic acid (PFNA), and perfluoroundecanoic acid (PFUnDA) increased during 1952–2009. The temporal trends for PFASs in Lake Hazen and Lake B35 sediments are consistent with the continuous annual delivery of PFASs to the Arctic of Canada. Temporal trends in sediment cores appear to follow historical market changes in PFAS manufacturing inventory. The doubling time of PFAS fluxes are faster in Lake Hazen sediments than Lake B35 sediments. In Lake Hazen, this may be attributed to the enhanced delivery of sediment and historically-archived PFASs promoted by climate-induced glacier melting in the Lake Hazen watershed post-

* Corresponding author.
E-mail addresses: john.macinnis@mun.ca (J.J. MacInnis), igor.lehnherr@utoronto.ca (I. Lehnherr), derek.muir@canada.ca (D.C.G. Muir), rquinlan@yorku.ca (R. Quinlan), amila.desilva@canada.ca (A.O. De Silva).

https://doi.org/10.1016/j.scitotenv.2019.02.210

2005. Exponentially increasing PFAS temporal trends in High and Low Arctic lakes in Canada stress the importance of developing effective global regulatory policies for PFAS manufacturing and highlights the potential for climate change-induced contaminant release from melting glaciers in the Arctic.

1. Introduction

Perfluoroalkyl substances (PFASs) are anthropogenic pollutants that are environmentally persistent, some of which have bioaccumulative properties (Ahrens et al., 2016; Butt et al., 2010; Campo et al., 2016). Perfluoroalkane carboxylic acids (PFCAs; $(F(CF_2)_{n+1}CO_2H)$ and perfluoroalkane sulfonic acids (PFSAs; $(F(CF_2)_{n+1}SO_3H)$, collectively known as perfluoroalkyl acids (PFAAs) are major classes of PFASs. PFCAs are manufactured by electrochemical fluorination (ECF) and fluorotelomerization (FT), whereas PFSAs are manufactured by ECF (Buck et al., 2011). PFCAs are used as processing aids in the manufacture of fluoropolymers and surface treatments, which are used for numerous applications such as oil and water repellency, and durability (Buck et al., 2011; Wang et al., 2014b). PFSAs are used as active ingredients in aqueous-film-forming-foams (AFFF) and mist suppressants during electroplating (Wang et al., 2017).

Historical PFAS manufacturing using ECF and FT shifted in response to industry phase-out initiatives. In 2002, the 3M Company phased-out its global production of perfluorooctyl-based (C8) chemistry using ECF due to concerns of environmental persistence and bioaccumulation, while perfluorooctanoic acid (PFOA) manufacturing was concurrently set in motion by DuPont using FT in the United States (US) (Wang et al., 2014b). In 2006, the USEPA invited six major fluorochemical manufacturers to participate in the PFOA Stewardship Program to further reduce PFAS emissions. Under this program, six major fluorochemical manufacturers agreed to reduce PFOA, long-chain PFCAs, and precursor emissions from facilities and products with full elimination by 2015 (USEPA, 2006). Several manufacturers committed to reduce or discontinue C8-based chemistry, however, several countries resume C8-based manufacturing. For example, estimated consumption of ammonium/sodium perfluorooctanoate for the manufacturing of polytetrafluoroethylene has increased in China, India, Poland and Russia from 248 to 347 kt $year^{-1}$ during 2006–2015, but decreased in Japan, Western Europe and the US from 320 to 200 kt $year^{-1}$ during 2006–2015 (Wang et al., 2014b). Similarly, China was a large-scale producer of perfluorooctane sulfonyl fluoride (POSF) post-2002, with estimated production volumes ranging from 50–250 and 100–250 tons $year^{-1}$ during 2003–2008 and 2008–2015, respectively (Wang et al., 2017). The global phase-out of C8-based chemistry and long-chain PFCAs promoted a recent shift toward the manufacturing of PFAS alternatives. For example, dodecafluoro-3H-4,8-dioxanonanoic acid (ADONA), a perfluoropolyether carboxylic acid, is a replacement for ammonium perfluorooctanoate and is regulated by the European Union REACH initiative with a tonnage band of 1–10 t per annum (ECHA, 2018; Gordon, 2011). Other PFAS alternatives include chlorinated polyfluorinated ether sulfonic acids (Cl-PFESAs), such as 9-chlorohexadecafluoro-3-oxanonane-1-sulfonic acid (6:2 Cl-PFESA) and 11-chloroeicosafluoro-3-oxaundecane-1-sulfonic acid (8:2 Cl-PFESA), which are major components of F-53B (Liu et al., 2017). F-53B is a mist suppressant replacement for PFOS during metal plating in China (Wang et al., 2013), with a reported usage of 20–30 tons during 2009 (Shi et al., 2015). It is expected that sustained manufacturing will contribute to global emissions of legacy and alternative PFASs in the environment.

The detection of PFASs in pristine remote environments, such as the Arctic demonstrates long-range transport (Butt et al., 2010; MacInnis et al., 2017; Stock et al., 2007; Yeung et al., 2017). PFAS deposition in Arctic regions is possible through the long-range atmospheric transport of aerosols such as sea spray, and the long-range atmospheric transport and oxidation of volatile precursors such as FTOHs and perfluoroalkane sulfonamido substances (Ellis et al., 2003; MacInnis et al., 2017; Pickard et al., 2017; Young et al., 2007).

Environmental archives are used to reconstruct historical periods of PFAS deposition. For example, wildlife tissue bank archives demonstrated PFAS temporal trends in livers from polar bears (*Ursus maritimus*) (Rigét et al., 2013; Smithwick et al., 2006) and ringed seals (*Phoca hispida*) (Rotander et al., 2012). Recently, a continuous air sampling campaign from 2006 to 2014 in Alert, Nunavut (82° N) demonstrated increasing temporal trends for PFAS concentrations on particles (Wong et al., 2018).

There are challenges associated with long-term environmental monitoring. Annual sampling for tissue banks or other long-term environmental monitoring is costly and can be logistically challenging for storage integrity. Furthermore, many tissue archives and monitoring datasets are not able to capture emissions during the onset of PFAS manufacturing in the 1950s (Braune and Letcher, 2013; Dassuncao et al., 2017; Pickard et al., 2017; Reiner et al., 2011; Rigét et al., 2013; Smithwick et al., 2006; Wong et al., 2018), which is useful for establishing and interpreting long-term chronological records of PFAS deposition in the environment. Another challenge with quantifying temporal trends includes changes in analytical methodology over time, which can affect inter-annual comparisons. To circumvent these challenges, chronological records of PFAS deposition determined using sediment and ice cores are advantageous because they can be collected during a single sampling excursion and analyzed using the same analytical methods with fine temporal resolution (MacInnis et al., 2017; Pickard et al., 2017). Sediment core analyses demonstrated chronological records of PFAS deposition in Tokyo Bay, (Ahrens et al., 2009; Zushi et al., 2010) High Arctic lakes, (Stock et al., 2007) and the Canadian Rocky Mountains (Benskin et al., 2011). In recent years, knowledge of historical PFAS emission inventories improved based on industry data (Wang et al., 2017; Wang et al., 2014a, 2014b) which is valuable for comparison of temporal trends in environmental samples.

In this study, chronological records of PFAS deposition are determined using sediment cores collected from the High Arctic, in the Lake Hazen watershed on northern Ellesmere Island at 82° N, and in the Low Arctic, in the Lake B35 watershed near Hudson Bay at 64° N. The primary objective of this study is to elucidate the role of long-range atmospheric transport and deposition on PFAS contaminant trends in the Arctic Archipelago. Lake Hazen is suitable in this regard because it is north of 75° N on Ellesmere Island and is far from local human contamination. In addition, the Lake Hazen watershed is unique compared to other watersheds in the High Arctic of Canada in that it receives substantial glacier inputs, providing a unique opportunity to examine PFAS deposition trends in the context of climate warming and the accelerated release of historically-archived (i.e. stored in glacier ice) PFASs. The size and accessibility of Lake Hazen are also contributing reasons for selection in this study. Lake B35 is selected also as an Arctic site, but in contrast to Lake Hazen due to the lower latitude, closer proximity to human settlements, and location on mainland Canada. Lake B35 is also of interest to fill a current data gap for PFAS deposition in the Low Arctic of Canada at 64° N and examine the relationship between climate warming and PFAS deposition in sediments from the Baker Lake region. We present the first chronological record of PFAS deposition in sediments north of 75° N and the most temporally-resolved chronological records of PFAS deposition in sediments from the Arctic of Canada.

2. Materials and methods

2.1. Study area description

Lake Hazen is the largest lake by volume north of the Arctic Circle and is located in Quttinirpaaq National Park on Ellesmere Island, Nunavut, Canada (supporting information (SI), Section S1, Table 1). The hydrological budget of Lake Hazen is dominated by glacial meltwater inputs and the lake is drained by the Ruggles River into Chandler Fiord (Lehnherr et al., 2018).

Lake B35 is a small lake approximately 6 km east of the community of Baker Lake, located near the geographic center of Canada (Section S1, Table 1). The hydrological budget of Lake B35 is dominated by surface runoff and thaw (i.e. permafrost) inputs. Lake B35 is drained into Prince River.

2.2. Sampling

Two intact sediment cores were collected on 30 May 2012, while the lake was fully ice-covered, from the deep trench (262 m deep) in Lake Hazen at 81.84° N, 70.51° W using a UWITEC gravity corer (http://www.uwitec.at/html/frame.html) with an 8.6 cm inner diameter polyvinyl chloride tube to determine dating chronology and PFAS deposition profiles. Further details of the Lake Hazen sediment core sampling method can be found in Lehnherr et al. (2018). Cores were extruded and sectioned in the Lake Hazen field laboratory at 0.5 cm (0–15 cm) and 1 cm (15–38 cm) intervals the same day. Each section was placed into polypropylene (PP) screw capped jars, frozen immediately on-site in a propane-powered freezer, and kept frozen until analyzed. Samples were transported to the Canada Centre for Inland Waters (CCIW), Burlington, Ontario for dating and analysis. An intact sediment core of 20 cm length was collected from the eastern basin of Lake B35 on 28 June 2009, at a mid-basin depth of 1.3 m, also using a UWITEC corer. The core was sectioned at 0.5 cm intervals up to 10 cm depth and stored in PP jars for transport and analysis at CCIW, Burlington, ON.

2.3. Sample extraction

Sediments were extracted according to Weber et al. (2017) with a few modifications. Briefly, 0.5 to 1 g of freeze-dried sediment was spiked with internal standard, consisting of isotopically labeled PFASs (Table S1) and subjected to an ultrasonic-assisted basicified methanolic extraction. After triplicate extraction and centrifugation, the supernatants were combined and taken to dryness using nitrogen gas. Residues were reconstituted in acidified methanol and heated before further concentration by nitrogen to a final 1.0 mL volume. A second suite of isotopically labeled standards was added before analysis to monitor matrix effects (Table S1). PFAS concentrations in sediment are blank, recovery, and matrix-corrected. Matrix effects are determined by comparing the peak area of isotopically labeled PFAS standards added after the extraction to the peak areas of PFASs in a solvent standard at equivalent concentrations. Analysis was by ultra-high performance liquid chromatography-tandem mass spectrometry (UPLC-MS/MS). Further details of chemicals, sediment extraction procedure, and QA/QC parameters are presented in the SI (Sections S2–S4, Tables S1–S2).

2.4. Instrumental analysis

All extracts were analyzed on an Acquity UPLC I class liquid chromatograph coupled to a XEVO TQ-S tandem mass spectrometer operated in electrospray negative ionization mode (Waters Corporation, Massachusetts, USA) as per previous methods (MacInnis et al., 2017; Pickard et al., 2017). PFASs were separated on an Acquity UPLC® BEH C18 (2.1 × 100 mm, 1.7 μm) stationary phase (Waters Corporation, Massachusetts, USA) using a 0.1 mM ammonium acetate water-methanol gradient. Details of the UPLC-MS/MS method are presented in the SI (Tables S1, S3–S4).

2.5. Sediment dating

Sectioned sediment core sub-samples were freeze-dried, ground, and treated to polonium distillation for alpha counting analysis. ^{137}Cs was determined by gamma spectroscopy for 47 h/sample using a high purity germanium spectrometer (DSPec, Ortec instruments) at Canada Centre for Inland Waters, Burlington, Canada. Dating and sedimentation rates are based on unsupported ^{210}Pb results using the Constant Rate of Supply (CRS) model (Appleby and Oldfield, 1978). Unsupported ^{210}Pb corresponds to the atmospheric fallout of ^{210}Pb that is incorporated into lake sediments resulting from the diffusion and subsequent decay of ^{222}Rn from soils (Appleby, 1998). The CRS model is chosen for sediment dating in this study because it provides robust dating accuracy by permitting changes in sedimentation rates over time (Appleby and Oldfield, 1978). The Lake Hazen dating was confirmed using the distinctive ^{137}Cs peak at 15.5 cm indicative of atmospheric nuclear weapons testing in the early 1960s. The Lake B35 dating was confirmed using ^{210}Pb profiles only. ^{137}Cs and ^{210}Pb profiles for Lake Hazen and Lake B35 are presented in the SI (Fig. S1). Sedimentation rates range from 0.047 to 6.659 (mean 0.922, median 0.389) g cm^{-2} year^{-1} in Lake Hazen during 1923–2011 and 0.011–0.015 (mean 0.013) g cm^{-2} year^{-1} in Lake B35 during 1940–2009. The limitations of High Arctic sediment sampling are discussed in the SI (Section S5, Fig. S2).

2.6. Data treatment

The limits of detection (LOD) and quantitation (LOQ) are designated as the concentration corresponding to signal-to-noise ratios (S/N) of 3 and 10 and are presented in Tables S5–S6. S/N ratios are calculated by dividing analyte peak height by the standard deviation of a solvent blank across homologue-specific retention time windows, as per a previous method (MacInnis et al., 2017). PFASs with detection frequencies <50% (i.e. C_4-C_6, C_{12}-C_{14}, C_{16} PFCAs; C_6, C_7, C_{10} PFSAs; PFECHS, FOSA, ADONA, 8-Cl-PFOS, 6:2 Cl-PFESA, and 8:2 Cl-PFESA) are excluded from temporal trend analyses. For all other PFASs (i.e. C_7-C_{11} PFCAs; C_4 and C_8 PFSAs), temporal trends are determined using fluxes derived from sediment concentrations equal to or greater than the LOD (Tables S5–S6). PFAS sedimentation flux (F_{sed}) is calculated according to $F_{sed} = C_{sed} \cdot R_{sed}/FF$, where C_{sed} is the concentration of PFASs in sediment (ng g^{-1} dry weight, dw), R_{sed} is the sedimentation rate estimated from the CRS model (g cm^{-2} year^{-1}), and FF is the focusing factor, as described by Yeung et al. (2013). Focusing factors of 11 and 1.2 are determined for Lake Hazen and Lake B35 sediments, respectively, according to FF = $^{210}Pb_{sed}/^{210}Pb_{soil}$, where $^{210}Pb_{sed}$ is the unsupported ^{210}Pb

Table 1
An overview of the Lake Hazen and Lake B35 study areas.

Site	Latitude (°N)	Longitude (°W)	Lake area (km^2)	Catchment area (km^2)	Catchment: lake area ratio	Lake depth (m)	Annual precipitation (mm)
Lake Hazen	81° 49′	70° 42′	540	7516	14	267	95[a]
Lake B35	64° 11′	95° 32′	0.0538	1.40	26	1.3[c]	250[b]

[a] Thompson, 1994.
[b] Environment and Climate Change Canada, 2018.
[c] Corresponds to the mid-basin depth due to unknown bathymetry in this lake.

inventory in sediment, and $^{210}Pb_{soil}$ is the local inventory of unsupported ^{210}Pb in soil due to atmospheric fallout, as reported by Lockhart et al. (1998). Statistical analysis on natural log-transformed sediment flux is performed using StatPlus:mac (V6), with a critical value set to 5% (i.e. $\alpha < 0.05$) for linear regression, Spearman (ρ), and Pearson (r) correlation analysis. Doubling times (t_2) are calculated for PFASs displaying first-order kinetics in sediment according to $t_2 = \ln(2)/k$, where k is the first order rate constant with units ($year^{-1}$) obtained from the slope of the linear regression of natural log-transformed PFAS flux (ng m^{-2} $year^{-1}$) versus time (year). The sum of PFAS concentrations (ΣPFAS) corresponds to the sum of all detected PFASs equal to or greater than homologue LOD at each depth (i.e. concentrations <LOD were assigned a value of 0).

3. Results and discussion

3.1. Composition of PFASs in sediments

Thirteen PFASs are detected in Lake Hazen sediments, including C_6-C_{13} PFCAs, C_4, C_6, C_8 PFSAs, PFECHS, and FOSA (Table S5). The most consistently detected PFASs in all Lake Hazen sediments are PFOA, PFDA, PFBS, PFOS. Several PFASs are only detected frequently at specific depth intervals in Lake Hazen sediments. For example, PFNA occurs in 3.25–9.25 cm (2002–2009 CE), PFUnDA in 6.25–13.75 cm (1987–2006 CE), PFDoDA in 7.25–9.75 cm (2000–2005 CE), and PFTrDA in 6.25–10.75 cm (1998–2006 CE, Fig. 1). The detection frequencies of other PFASs including PFHxA, PFHpA, PFECHS, PFHxS, and FOSA are low and inconsistent in Lake Hazen sediments. The highest concentrations of C_6-C_9 PFCAs and C_4, C_6, C_8 PFSAs in Lake Hazen sediments occur in 0.25–2.25 cm (all 5 sections corresponding to 2011 CE). Diverting from this trend, maximum concentrations of PFDA and FOSA occur at 9.25 cm (2002 CE), whereas maximum concentrations of PFUnDA, PFDoDA, and PFTrDA occur at 7.75 cm (2004 CE). ΣPFAS concentrations range from 0.006 to 0.161 ng g^{-1} dw, with a maximum concentration at 9.25 cm (2002 CE, Fig. 1). The sum of PFCA concentration (ΣPFCA) exceeds PFSAs, comprising 64 ± 3% (mean ± standard error, SE) of all the PFASs quantified throughout the sediment core.

Seven PFASs are detected in Lake B35 sediments, including C_7-C_{11} PFCAs, as well as C_4 and C_8 PFSAs (Table S6, Fig. 1). PFOA and PFNA are detected in all/most sediments in 0.25–3.75 cm (1963–2009 CE), whereas PFHpA, PFDA, and PFUnDA are detected in most sediments in 0.25–2.75 cm (1986–2009 CE). PFOS is only detected at 0.25 cm (2009 CE) and PFBS in 1.25–2.75 cm (1986–2002 CE). The highest individual concentrations of C_7-C_{11} PFCAs and PFOS in Lake B35 sediments

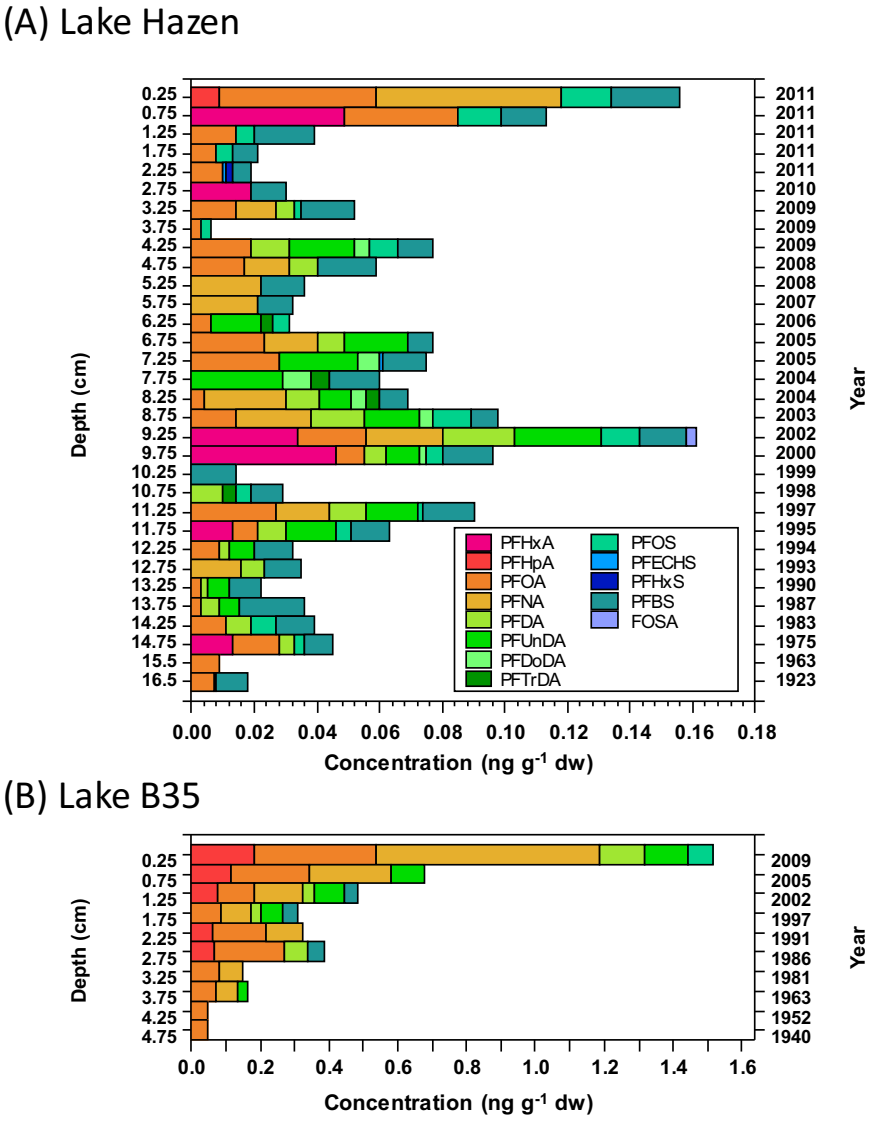

Fig. 1. Composition profiles of PFASs sediment cores using concentrations (ng g^{-1} dw) versus midpoint depth (left y-axis, cm) and year (right y-axes) in A) Lake Hazen and B) Lake B35. Legend applies to both panels. ADONA, 8-Cl-PFOS, 6:2 Cl-PFESA, and 8:2 Cl-PFESA were all <LOD and omitted from this figure.

occur at 0.25 cm (2009 CE). ΣPFAS concentrations range from 0.044 to 1.52 ng g^{-1} dw, with a maximum concentration at 0.5 cm (2009 CE, Fig. 1). ΣPFCA concentration is 96 ± 2% of all PFASs quantified throughout the sediment core.

The composition profiles for PFASs in Lake Hazen and Lake B35 sediments demonstrate that these regions are impacted by different emission sources. For example, PFSAs are detected more frequently in Lake Hazen sediments than Lake B35 sediments, indicating that ECF-based sources are more impactful in the Lake Hazen region. The general absence of PFHxS in sediments from Lake Hazen and Lake B35 (Fig. 1) is noteworthy given that PFHxS is a co-contaminant in AFFF formulations with PFBS and PFOS (Backe et al., 2013; D'Agostino and Mabury, 2017) and has a higher partitioning coefficient (i.e. K_d) in sediment than PFBS (Zhu et al., 2014) (Fig. 1). As such, the low detection frequency of PFHxS relative to PFBS and PFOS in Lake Hazen and Lake B35 sediments indicates that PFBS and PFOS are derived from a non-AFFF source. On the other hand, it is possible that the low detection frequency of PFHxS in Lake Hazen and Lake B35 sediments indicates that PFHxS emissions from the product life-cycles of perfluorohexane sulfonyl fluoride (PHxSF) and POSF-based products are limited in these regions (Boucher et al., 2018).

3.2. Temporal trends in sediment

The Lake Hazen and Lake B35 sediment cores correspond to depositional periods from 1923–2011 and 1940–2009, respectively. Low ΣPFAS flux in sediments prior to the 1950s is regarded as a period that precedes large-scale PFAS manufacturing (Benskin et al., 2011) (Section S4). PFAS deposition prior to the 1950s is omitted from temporal trend analysis to portray the influence of large scale manufacturing on the environmental loading of PFASs in Lake Hazen and Lake B35 (Fig. 2).

In Lake Hazen, PFBS, PFOA, PFDA, and PFOS have detection frequencies >50%, and thus are used to analyze temporal trends. Exponentially increasing fluxes ($p < 0.01$) are observed during 1963–2011, with doubling times corresponding to 6.9 (95% confidence interval; 5.3–11) years for PFOA, 6.9 (4.9–11) years for PFDA, 6.3 (4.1–11) years for PFOS, and 7.7 (5.8–11) years for PFBS (Table S7). Exponentially increasing fluxes are also observed in Lake B35 during 1952–2009, with doubling times corresponding to 14 (7.7–110) years for PFHpA, 21 (13–49) years for PFOA, 14 (8.7–69) years for PFNA, and 19 (15–25) years for PFUnDA (Table S7). A comparison of doubling times in Lake Hazen and Lake B35 sediments with PFAS trends in other sediment and wildlife is presented in Table 2 and discussed in Section S6. The doubling time for PFOA is within the range of doubling times for PFOA in a sediment core collected from Lake Oesa in the Canadian Rocky Mountains fluxes from 1957 to 2008 (Table 2). Interestingly, FOSA and long-chain PFCAs, such as PFDoDA and PFTrDA were detected frequently in sediments from Lake Oesa and Lake Opabin, but not in sediments from Lake Hazen and Lake B35. Higher detection frequencies of long-chain PFCAs and FOSA in Lake Oesa and Lake Opabin, located at altitudes >2000 m and 51° N in western Canada, suggest these regions are impacted by different air mass pollution than Lake Hazen and Lake B35.

Annual fluxes of PFOA from 1963–2008 and 1952–2009 in Lake Hazen and Lake B35 sediment cores, respectively, are similar to PFOA fluxes in Lake Oesa located in the Western Canada Rocky Mountains during 1967–2008 (Table 3) (Benskin et al., 2011). In contrast, annual fluxes of PFOA and PFOS in Lake Hazen and Lake B35 sediments during 1963–2008 and 1952–2009, respectively are approximately 100 and 200 times, respectively, lower than annual fluxes in Lake Ontario sediments (Table 3) (Yeung et al., 2013). It is noteworthy that the magnitude of PFOS deposition in Lake Ontario is greater than Lake Hazen, despite having lower sedimentation rates relative to Lake Hazen, which highlights the impact of local anthropogenic activity in the Lake Ontario watershed on elevating PFOS sediment concentrations relative to Lake Hazen and Lake B35 (Table 3).

The doubling times for PFAAs are faster in Lake Hazen sediments than Lake B35 sediments. A recent study by Lehnherr et al. (2018)

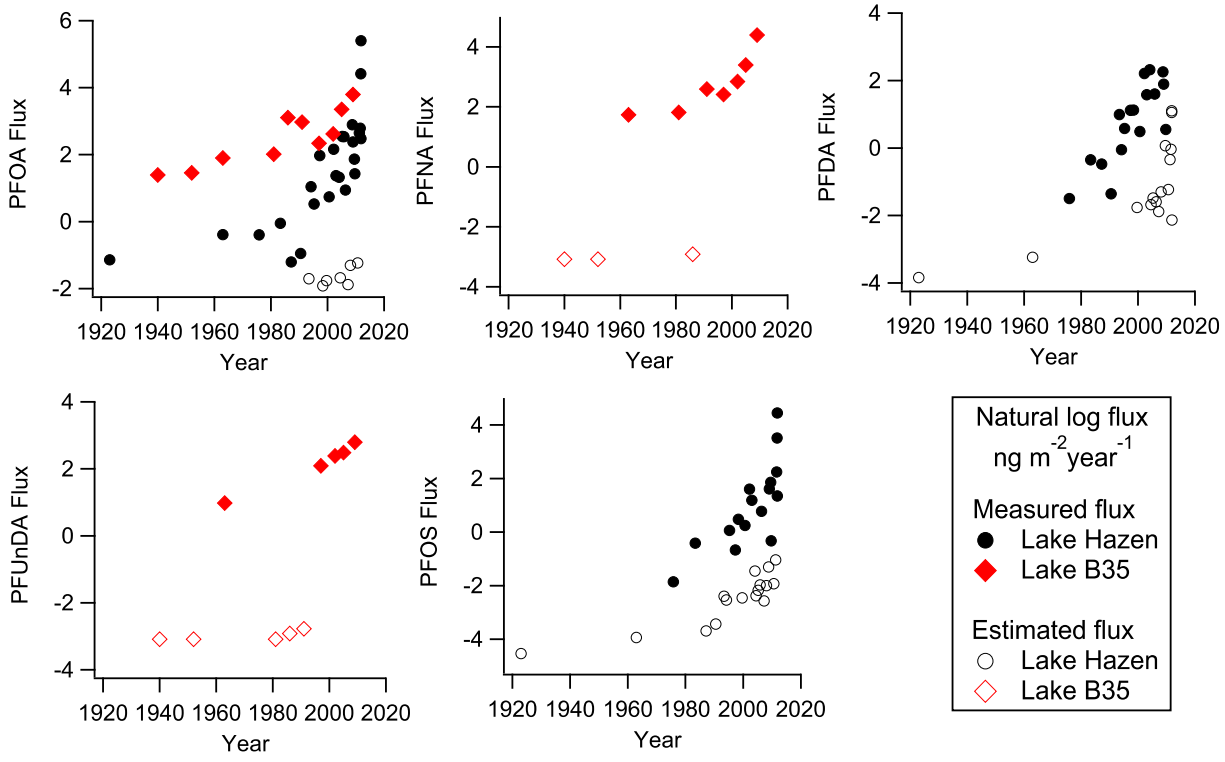

Fig. 2. Natural log-transformed PFAS fluxes (ng m^{-2} $year^{-1}$) into Lake Hazen (filled black circles, 1923–2011), and Lake B35 (filled red squares, 1940–2009) sediments. Fluxes were estimated at Lake Hazen (unfilled circles) and Lake B35 (unfilled squares) using substituted sediment concentrations equal to LOD.

Table 2
Comparison of doubling times (and 95% confidence interval) of PFAS fluxes in Lake Hazen and Lake B35 sediments with reported sediment and wildlife bank tissue archives. Doubling times for all sites were calculated using only detected concentrations.

Location	Lake Hazen, Nunavut, Canada	Lake B35, Nunavut, Canada	Lake Oesa, Canadian Rocky Mountains[a]	Lake Ontario, Station 1034[b]	Baffin Island, Nunavut, Canada[c]	Barrow, Alaska, USA[c]	Qeqertarsuaq, West Greenland[d]	Prince Leopold Island Nunavut, Canada[e]
	Sediment core	Sediment core	Sediment core	Sediment core	Polar bear liver	Polar bear liver	Ringed seal liver	Northern fulmar eggs
Period	1963–2011	1952–2009	1957–2008	1952–2005	1972–2002	1972–2002	1982–2006	1975–2011
Doubling time (years)								
PFHpA		14 (7.7–110)						
PFOA	6.9 (5.3–11)	21 (13–49)	11 (7.7–35)	9.9 (8.7–14)	7.3 (4.5–10.1)			
PFNA		14 (8.7–69)			3.6 (2.7–4.5)	5.6 (4.7–6.5)		5.3 (4.3–6.9)
PFDA	6.9 (4.9–11)				4.2 (3.2–5.2)	6.7 (5.0–8.4)	9.9 (6.9–35)	8.7 (5.8–17)
PFUnDA		19 (15–25)	8.7 (6.9–14)		4.1 (2.7–5.5)	6.1 (5.0–7.2)	8.7 (6.9–17)	5.3 (3.8–8.7)
PFBS	7.7 (5.8–11)							
PFOS	6.3 (4.1–11)			14 (11–17)	9.8 (4.7–14.9)	13.1 (9.1–17.1)		

[a] Benskin et al., 2011.
[b] Yeung et al., 2013.
[c] Smithwick et al., 2006.
[d] Rigét et al., 2013.
[e] Braune and Letcher, 2013.

noted climate-warming in the Lake Hazen watershed resulted in large scale mass losses from glaciers driving inputs of sediment, organic carbon, mercury, and organochlorine pesticides (OCPs) into the Lake Hazen watershed. Glaciers are also repositories for atmospheric PFAS deposition, consistent with observations in ice cores from the High Arctic of Canada (MacInnis et al., 2017; Pickard et al., 2017; Young et al., 2007), Svalbard (Kwok et al., 2013), and the European Alps (Kirchgeorg et al., 2013). Thus, it is reasonable to hypothesize that melting glaciers vector PFASs into Lake Hazen. In Longyearbyen, Svalbard, Norway (78° N) PFAS concentrations in glacier meltwater were an order of magnitude higher than concentrations in glacial surface snow (Kwok et al., 2013). Kwok et al. (2013) postulated that climate-warming accelerated glacier melting, resulting in the coalescence of multi-decadal meltwater enriched in PFASs.

To investigate the effect of melting glaciers on PFAS deposition, annual glacier meltwater discharge in the Lake Hazen watershed is correlated to fluxes of PFASs in Lake Hazen sediments during 1963–2011. Correlation analysis of natural log-transformed PFAS fluxes and annual glacial meltwater discharge suggests that PFOA ($r = 0.65$, $p = 0.01$), PFBS ($r = 0.55$, $p = 0.02$), and PFOS ($r = 0.69$, $p = 0.02$) deposition in Lake Hazen sediments is impacted by glacier melting. Climate-induced glacial melting promotes greater rates of sediment accumulation in Lake Hazen via increasing riverine inputs into the lake (Lehnherr et al., 2018). As such, the variability in glacier meltwater discharge is reflected in the rates of sediment accumulation, particularly post-2005 when glacier melting is most variable. For example, fluxes of PFOA in Lake Hazen sediments are notably consistent with glacier meltwater discharge post-2005, suggesting the increased delivery of sediment and glacier meltwaters post-2005 increased the input of historically-archived and surface runoff inputs of PFOA into Lake Hazen (Fig. 3). Similar observations were reported by Lehnherr et al. (2018), whereby higher concentrations of legacy OCPs were observed in a Lake Hazen sediment core post-2000 in response to enhanced glacier melting. In contrast, fluxes of PFDA in Lake Hazen sediments are not correlated with annual glacier meltwater discharge ($r = 0.35$, $p = 0.20$), which may suggest that the delivery of PFDA into Lake Hazen is governed by snowmelt in the surrounding catchment. Taken together, melting glaciers in the Lake Hazen watershed are vectors of sediment and historically-archived PFASs, particularly post-2005, which can be used to corroborate the faster increasing depositional trends and impact of climate warming on PFAS deposition in Lake Hazen sediments. In contrast, climate analysis in the Baker Lake region, which is close to Lake B35, indicates that mean annual temperature (mean ± SE, −11.8 ± 0.2 °C) and precipitation (253 ± 7 mm) was fairly constant during 1952–2009 (Environment and Climate Change Canada, 2018), suggesting these climate factors do not account for the increasing PFAS deposition in Lake B35 sediment.

The increasing temporal trends for PFASs suggest that historical emissions from FT and ECF-based sources impact PFAS deposition in Lake Hazen and Lake B35 sediments. Isomer profiling is an effective tool for tracking FT and ECF-based sources (Benskin et al., 2011; Johansson et al., 2018), however, this approach is not feasible in this study due to the low concentrations of PFASs in sediments, particularly in Lake Hazen. To investigate the influence of FT and ECF manufacturing on PFAS deposition in Lake Hazen and Lake B35, PFAS fluxes in sediments are correlated with estimated annual production volumes of FT-based products and POSF. In Lake Hazen, fluxes of PFOA, PFDA, and PFBS are strongly correlated with FT-based production volumes during 1963–2005 ($\rho \geq 0.65$, $p < 0.01$). Similarly, strong correlations are observed between FT-based production volumes and all PFCA fluxes in Lake B35 during 1963–2009 ($\rho \geq 0.72$, $p < 0.05$). These observations suggest FT manufacturing is a dominant historic source of PFCAs to the

Table 3
Comparison of mean PFAS mass sedimentation fluxes (ng m^{-2} $year^{-1}$) in Lake Hazen and Lake B35 sediments to Lake Ontario sediment sediments. Sedimentation rates are expressed in g cm^{-2} $year^{-1}$. Range of fluxes are presented in parentheses.

Location	Lake Hazen, Nunavut, Canada	Lake B35, Nunavut, Canada	Lake Oesa, Canadian Rocky Mountains	Lake Ontario, Canada Station 1004
Matrix	Sediment core	Sediment core	Sediment core	Sediment core
Period	1963–2008	1952–2009	1957–2008	1953–2004
Sedimentation Rates	0.050–6.659	0.011–0.015	0.029–0.058	0.025–0.038
Analyte	Flux	Flux	Flux	Flux
PFOA	5.0 (<0.29–18)	21 (5.2–54)	9.5 (<LOD-29)	683 (<6–1139)
PFOS	1.7 (<0.039–4.9)	(<0.11–10)	<LOD	3087 (292–10,410)

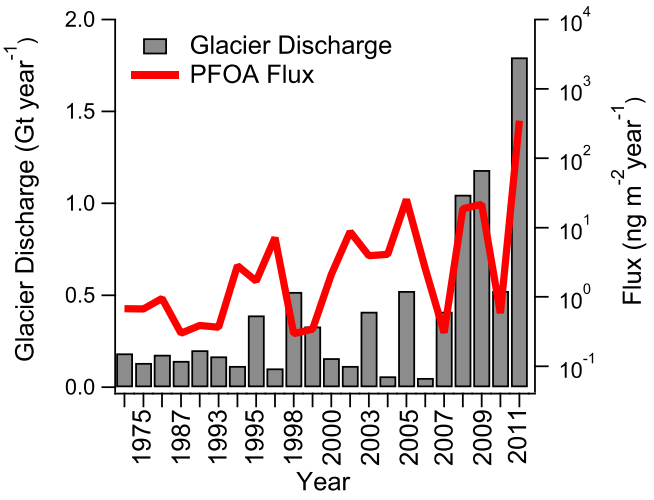

Fig. 3. Comparison of glacier meltwater discharge (Gt year^{-1}, left y-axis, gray bars) in the Lake Hazen watershed and PFOA fluxes (ng m^{-2} year^{-1}, right y-axis, red line) in the Lake Hazen sediment core versus time (bottom x-axis, 1963–2011). PFOA fluxes were estimated for Lake Hazen data <LOD by using LOD-substituted concentrations for flux calculations.

Arctic of Canada. In contrast, PFAS fluxes in Lake Hazen and Lake B35 sediments are not correlated with estimated POSF production volumes (Table S8). Weak correlations between PFSA fluxes and POSF production volumes indicate that PFSA deposition in Lake Hazen and Lake B35 sediments is not representative of the production trends for POSF.

The composition profiles of PFASs in Lake Hazen and Lake B35 sediments are generally consistent with regulatory phase-out initiatives and historical market changes in PFAS manufacturing. For example, the low detection frequency of PFOS and FOSA in Lake Hazen sediments post-2003 is consistent with the global phase-out of perfluorooctane sulfonyl-based chemistries by the 3M Company in 2002, whereas the high detection frequency of C_8-C_{12} PFCAs in Lake Hazen sediments during 2003–2005 is consistent with emerging global FT manufacturing using C8-based chemistries (Fig. 1). Similarly, the low detection frequency of C_{10}-C_{13} PFCAs in Lake Hazen sediments post-2006 is consistent with reductions of C8-based emissions by FT manufacturers participating in the USEPA PFOA Stewardship Program (Fig. 1). The detection of PFHxA in Lake Hazen sediments during 2010 and 2011 may also provide evidence of global PFAS manufacturing shifts toward shorter-chain chemistries in recent years due to global phase-out initiatives. However, it is possible that resurgences in global PFAS emissions impact environmental inventories in Lake Hazen and Lake B35 sediments. For example, the detection long-chain PFCAs and PFOS in Lake Hazen and Lake B35 sediments post-2006 may provide historical evidence of global emission resurgences due to the sustained production of PFASs by C8-based chemistry (Ruan et al., 2010), or reflects emissions during the life-cycle of PFAS products manufactured prior to industry phase-out initiatives. The absence of PFAS alternatives such as 6:2 and 8:2 Cl-PFESA, and ADONA in Lake Hazen and Lake B35 sediments indicates that emissions from the manufacturing of PFAS alternatives are not impactful in the Arctic of Canada. These observations are in contrast to observations reported by Gebbink et al. (2016), whereby 6:2 Cl-PFESA was detected in livers of polar bears, ringed seals, and killer whales in East Greenland during 2012 and 2013. Similarly, 6:2 Cl-PFESA was measured in surface waters from rivers and lakes in China, the U.S., United Kingdom, Sweden, Germany, Netherlands, and South Korea during 2016 (Pan et al., 2018), demonstrating that PFAS alternatives are amenable to global dissemination. Future work should focus on the continued monitoring of legacy and novel PFAS alternatives in Lake Hazen and Lake B35 to evaluate the efficacy of industry phase-out initiatives and the impact of market changes on PFAS deposition in the Arctic of Canada.

3.3. Implications for PFAS deposition in the Arctic of Canada

The detection of PFASs in remote High and Low Arctic lakes in Canada corroborates evidence of long-range atmospheric transport. Some of the most compelling evidence for long-range transport is the detection of PFCAs in High Arctic ice caps, including Devon Island ice cap and Agassiz ice cap on Ellesmere Island, both sampled at 1800 m above sea-level (MacInnis et al., 2017; Pickard et al., 2017; Young et al., 2007). In recent studies, PFCA deposition on the Devon Ice Cap is governed by the long-range atmospheric transport and oxidation of volatile precursors (MacInnis et al., 2017; Pickard et al., 2017; Young et al., 2007). The Devon Ice Cap is located at 75° N, an intermediate latitude between Lake Hazen and Lake B35, implying that these lakes may be influenced by the same air masses as the Devon Ice Cap. To investigate this hypothesis, PFOA and PFOS fluxes from the Devon Ice Cap, Lake Hazen, and Lake B35 are compared (Figs. 4, S3). Overall, there is a general agreement for PFOA fluxes in Lake B35 (mean ± SE, 1981–2009, 21 ± 5 ng m^{-2} year^{-1}), and the Devon Ice Cap (1982–2009, 32 ± 3 ng m^{-2} year^{-1}). Interestingly, after 1997, PFOA flux in Lake B35 increased from 14 to 45 ng m^{-2} year^{-1} during 2002–2009, which is consistent with the gradual increase observed on the Devon Ice Cap from 16 to 41 ng m^{-2} year^{-1} during 2003–2008 (Fig. 4). In contrast, the magnitude of mean PFOA and PFOS fluxes in Lake Hazen was 11 and 3 times lower, respectively, than mean PFOA and PFOS fluxes observed on the Devon Ice Cap during 1983–2004 (Figs. 4, S3). The maximum flux of PFOA in Lake Hazen is observed during 2011 corresponding to 346 ng m^{-2} year^{-1} and was 19 times greater than the flux on the Devon Ice Cap during 2011. Interestingly, the maximum flux of PFOS observed during 2011 in Lake Hazen (133 ng m^{-2} year^{-1}) is similar to the maximum flux of PFOS reported on the Devon Ice Cap in 2013 (80.3 ng m^{-2} year^{-1}). PFOS was only detected in one sample from Lake B35 in 2009 (8.7 ng m^{-2} year^{-1}), possibly due to limited temporal resolution relative to Lake Hazen and

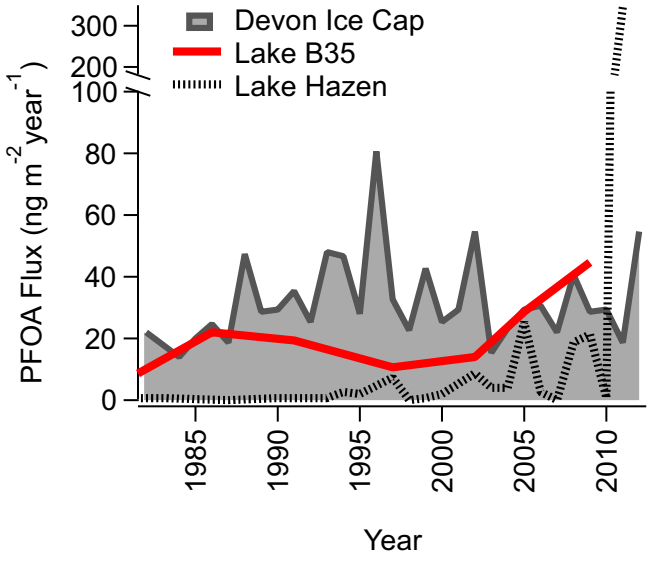

Fig. 4. Comparison of PFOA flux deposition (ng m^{-2} year^{-1}, y-axis) in Lake Hazen and Lake B35 sediment to an ice core from the summit of the Devon Ice Cap (Pickard et al., 2017) over a 1982–2011 temporal period. The PFOA mass flux for Lake Hazen, Lake B35, and the Devon Ice Cap is represented by a black dashed line, solid red line, and a gray-filled trace, respectively. PFOA flux was estimated for Lake Hazen data <LOD by using LOD-substituted concentrations for flux calculations.

the Devon Ice Cap but is consistent with the maximum flux observed on the Devon Ice Cap during 1982–2009 (9.57 ng m^{-2} $year^{-1}$).

The general consistency of PFOA deposition in Lake B35 and the Devon Ice Cap suggests these regions are impacted by similar source regions, predominantly via long-range atmospheric transport and deposition. The contrast observed for the magnitude of PFAS deposition during 2011 in Lake Hazen can be attributed to differences in sediment delivery driven by climate-induced glacier melting. It is likely that these study areas are influenced by both North American and Eurasian air masses to some extent given the prevalence of PFAS manufacturing in these countries. The importance of local emission sources on PFAS deposition is currently unknown in Lake Hazen and Lake B35, which may also contribute to environmental loading in these areas.

4. Conclusions

In this study, exponentially increasing temporal trends are observed for PFASs in High and Low Arctic lakes in Canada, which are consistent with historical market changes in PFAS manufacturing inventory. Faster doubling times of PFAS fluxes in Lake Hazen sediments demonstrates the potential for climate change-induced contaminant release from melting glaciers in the Arctic. The consistency of observations in this study with the Devon Ice Cap suggests the Arctic will continue to act as a sink for contemporary PFAS pollution in lower latitudes, which highlights the importance of developing effective global regulatory policy for PFASs.

Acknowledgements

We thank Charles Talbot (Environment and Climate Change Canada, ECCC) for assistance in sample collection of the Lake Hazen sediment core, Raymond Biastoch, Christopher Luszczek, and Andrew Medeiros (York University) for assistance in sample collection of the Lake B35 sediment core. We also thank Fan Yang (ECCC) for dating the Lake Hazen and Lake B35 sediment cores and Johan Wiklund for further refinements. This project was funded by the Polar Continental Shelf Program (Natural Resources Canada), the Natural Science and Engineering Research Council (NSERC), the Northern Contaminants Program (Indigenous and Northern Affairs Canada), and the Garfield Weston Foundation. NSERC (JJM) is acknowledged for a postgraduate scholarship.

Appendix A. Supplementary data

Additional details on sample handling and analysis, sediment dating, QA/QC parameters, PFAS concentration data. Supplementary data to this article can be found online at https://doi.org/10.1016/j.scitotenv.2019.02.210.

References

Ahrens, L., Yamashita, N., Yeung, L.W.Y., Taniyasu, S., Horii, Y., Lam, P.K.S., Ebinghaus, R., 2009. Partitioning behavior of per- and polyfluoroalkyl compounds between pore water and sediment in two sediment cores from Tokyo Bay, Japan. Environ. Sci. Technol. 43, 6969–6975. https://doi.org/10.1021/es901213s.

Ahrens, L., Gashaw, H., Sjöholm, M., Gebrehiwot, S.G., Getahun, A., Derbe, E., Bishop, K., Åkerblom, S., 2016. Poly- and perfluoroalkylated substances (PFASs) in water, sediment and fish muscle tissue from Lake Tana, Ethiopia and implications for human exposure. Chemosphere 165, 352–357. https://doi.org/10.1016/j.chemosphere.2016.09.007.

Appleby, P.G., 1998. Dating Recent Sediment by ^{210}Pb: Problems and Solutions, Stuk a-145. https://doi.org/10.1016/j.gie.2012.05.034.

Appleby, P.G., Oldfield, F., 1978. The calculation of lead-210 dates assuming a constant rate of supply of unsupported Pb-210 in the sediment. Catena 5, 1e8 (Catena 5, 1978).

Backe, W.J., Day, T.C., Field, J.A., 2013. Zwitterionic, cationic, and anionic fluorinated chemicals in aqueous film forming foam formulations and groundwater from U.S. military bases by nonaqueous large-volume injection HPLC-MS/MS. Environ. Sci. Technol. https://doi.org/10.1021/es3034999.

Benskin, J.P., Phillips, V., St. Louis, V.L., Martin, J.W., 2011. Source elucidation of perfluorinated carboxylic acids in remote alpine lake sediment cores. Environ. Sci. Technol. 45, 7188–7194. https://doi.org/10.1021/es2011176.

Boucher, J.M., Cousins, I.T., Scheringer, M., Hungerbühler, K., Wang, Z., 2018. Toward a comprehensive global emission inventory of C4–C10 perfluoroalkanesulfonic acids (PFSAs) and related precursors: focus on the life cycle of C6- and C10-based products. Environ. Sci. Technol. Lett. https://doi.org/10.1021/acs.estlett.8b00531.

Braune, B.M., Letcher, R.J., 2013. Perfluorinated sulfonate and carboxylate compounds in eggs of seabirds breeding in the Canadian Arctic: temporal trends (1975–2011) and interspecies comparison. Environ. Sci. Technol. 47, 616–624. https://doi.org/10.1021/es303733d.

Buck, R.C., Franklin, J., Berger, U., Conder, J.M., Cousins, I.T., De Voogt, P., Jensen, A.A., Kannan, K., Mabury, S.A., van Leeuwen, S.P.J., 2011. Perfluoroalkyl and polyfluoroalkyl substances in the environment: terminology, classification, and origins. Integr. Environ. Assess. Manag. 7, 513–541. https://doi.org/10.1002/ieam.258.

Butt, C.M., Berger, U., Bossi, R., Tomy, G.T., 2010. Levels and trends of poly- and perfluorinated compounds in the arctic environment. Sci. Total Environ. 408, 2936–2965. https://doi.org/10.1016/j.scitotenv.2010.03.015.

Campo, J., Lorenzo, M., Pérez, F., Picó, Y., la Farré, M., Barceló, D., 2016. Analysis of the presence of perfluoroalkyl substances in water, sediment and biota of the Jucar River (E Spain). Sources, partitioning and relationships with water physical characteristics. Environ. Res. 147, 503–512. https://doi.org/10.1016/j.envres.2016.03.010.

D'Agostino, L.A., Mabury, S.A., 2017. Certain perfluoroalkyl and polyfluoroalkyl substances associated with aqueous film forming foam are widespread in Canadian surface waters. Environ. Sci. Technol. https://doi.org/10.1021/acs.est.7b03994.

Dassuncao, C., Hu, X.C., Zhang, X., Bossi, R., Dam, M., Mikkelsen, B., Sunderland, E.M., 2017. Temporal shifts in poly- and perfluoroalkyl substances (PFASs) in North Atlantic pilot whales indicate large contribution of atmospheric precursors. Environ. Sci. Technol. 51, 4512–4521. https://doi.org/10.1021/acs.est.7b00293.

ECHA, 2018. Committee for Risk Assessment (RAC) Committee for Socio-economic Analysis (SEAC) Background Document. https://doi.org/10.1063/1.1809272.

Ellis, D.A., Martin, J.W., Mabury, S.A., Hurley, M.D., Sulbaek Andersen, M.P., Wallington, T.J., 2003. Atmospheric lifetime of fluorotelomer alcohols. Environ. Sci. Technol. 37, 3816–3820.

Environment and Climate Change Canada, 2018. Climate Normals 1981–2010 Baker Lake [WWW Document]. URL http://climate.weather.gc.ca/climate_normals/results_1981_2010_e.html?stnID=1709&lang=e&StationName=Baker+Lake&SearchType=Contains&stnNameSubmit=go&dCode=1&dispBack=1, Accessed date: 6 March 2018.

Gebbink, W.A., Bossi, R., Rigét, F.F., Rosing-Asvid, A., Sonne, C., Dietz, R., 2016. Observation of emerging per- and polyfluoroalkyl substances (PFASs) in Greenland marine mammals. Chemosphere 144, 2384–2391. https://doi.org/10.1016/j.chemosphere.2015.10.116.

Gordon, S.C., 2011. Toxicological evaluation of ammonium 4,8-dioxa-3H-perfluorononanoate, a new emulsifier to replace ammonium perfluorooctanoate in fluoropolymer manufacturing. Regul. Toxicol. Pharmacol. 59, 64–80. https://doi.org/10.1016/j.yrtph.2010.09.008.

Johansson, J.H., Shi, Y., Salter, M., Cousins, I.T., 2018. Spatial variation in the atmospheric deposition of perfluoroalkyl acids: source elucidation through analysis of isomer patterns. Environ. Sci. Process. Impact. https://doi.org/10.1039/c8em00102b.

Kirchgeorg, T., Dreyer, A., Gabrieli, J., Kehrwald, N., Sigl, M., Schwikowski, M., Boutron, C., Gambaro, A., Barbante, C., Ebinghaus, R., 2013. Temporal variations of perfluoroalkyl substances and polybrominated diphenyl ethers in alpine snow. Environ. Pollut. 178, 367–374. https://doi.org/10.1016/j.envpol.2013.03.043.

Kwok, K.Y., Yamazaki, E., Yamashita, N., Taniyasu, S., Murphy, M.B., Horii, Y., Petrick, G., Kallerborn, R., Kannan, K., Murano, K., Lam, P.K.S., 2013. Transport of perfluoroalkyl substances (PFAS) from an arctic glacier to downstream locations: implications for sources. Sci. Total Environ. 447, 46–55. https://doi.org/10.1016/j.scitotenv.2012.10.091.

Lehnherr, I., St. Louis, V.L., Sharp, M., Garnder, A., Smol, J., Schiff, S., Muir, D., Mortimer, C., Michelutti, N., Tarnocai, C., St. Pierre, K., Emmerton, C., Wiklund, J., Kock, G., Lamoureux, S., Talbot, C., 2018. The world's largest High Arctic lake responds rapidly to climate warming. Nat. Commun. 9, 1–9. https://doi.org/10.1038/s41467-018-03685-z.

Liu, Y., Ruan, T., Lin, Y., Liu, A., Yu, M., Liu, R., Meng, M., Wang, Y., Liu, J., Jiang, G., 2017. Chlorinated polyfluoroalkyl ether sulfonic acids in marine organisms from Bohai Sea, China: occurrence, temporal variations, and trophic transfer behavior. Environ. Sci. Technol. 51, 4407–4414. https://doi.org/10.1021/acs.est.6b06593.

Lockhart, W.L., Wilkinson, P., Billeck, B.N., Danell, R.A., Hunt, R.V., Brunskill, G.J., Delaronde, J., St. Louis, V., 1998. Fluxes of mercury to lake sediments in central and northern Canada inferred from dated sediment cores. Biogeochemistry 40, 163–173. https://doi.org/10.1023/A:1005923123637.

MacInnis, J.J., French, K., Muir, D.C., Spencer, C., Criscitiello, A., De Silva, A.O., Young, C.J., 2017. Emerging investigator series: a 14-year depositional ice record of perfluoroalkyl substances in the High Arctic. Environ. Sci. Process. Impact 19, 22–30.

Pan, Y., Zhang, H., Cui, Q., Sheng, N., Yeung, L.W.Y., Sun, Y., Guo, Y., Dai, J., 2018. Worldwide distribution of novel perfluoroether carboxylic and sulfonic acids in surface water. Environ. Sci. Technol. 52, 7621–7629. https://doi.org/10.1021/acs.est.8b00829.

Pickard, H.M., Criscitiello, A.S., Spencer, C., Sharp, M.J., Muir, D.C.G., De Silva, A.O., Young, C.J., 2017. Continuous non-marine inputs of per- and polyfluoroalkyl substances to the High Arctic: a multi-decadal temporal record. Atmos. Chem. Phys. Discuss. 1–25.

Reiner, J.L., O'Connell, S.G., Moors, A.J., Kucklick, J.R., Becker, P.R., Keller, J.M., 2011. Spatial and temporal trends of perfluorinated compounds in beluga whales (Delphinapterus leucas) from Alaska. Environ. Sci. Technol. 45, 8129–8136. https://doi.org/10.1021/es103560q.

Rigét, F., Bossi, R., Sonne, C., Vorkamp, K., Dietz, R., 2013. Trends of perfluorochemicals in Greenland ringed seals and polar bears: indications of

shifts to decreasing trends. Chemosphere 93, 1607–1614. https://doi.org/10.1016/j.chemosphere.2013.08.015.
Rotander, A., Kärrman, A., van Bavel, B., Polder, A., Rigét, F., Audunsson, G.A., Víkingsson, G., Gabrielsen, G.W., Bloch, D., Dam, M., 2012. Increasing levels of long-chain perfluorocarboxylic acids (PFCAs) in Arctic and North Atlantic marine mammals, 1984–2009. Chemosphere 86, 278–285. https://doi.org/10.1016/j.chemosphere.2011.09.054.
Ruan, T., Wang, Y., Wang, T., Zhang, Q., Ding, L., Liu, J., Wang, C., Qu, G., Jiang, G., 2010. Presence and partitioning behavior of polyfluorinated iodine alkanes in environmental matrices around a fluorochemical manufacturing plant: another possible source for perfluorinated carboxylic acids? Environ. Sci. Technol. 44, 5755–5761. https://doi.org/10.1021/es101507s.
Shi, Y., Vestergren, R., Zhou, Z., Song, X., Xu, L., Liang, Y., Cai, Y., 2015. Tissue distribution and whole body burden of the chlorinated polyfluoroalkyl ether sulfonic acid F-53B in crucian carp (*Carassius carassius*): evidence for a highly bioaccumulative contaminant of emerging concern. Environ. Sci. Technol. https://doi.org/10.1021/acs.est.5b04299.
Smithwick, M., Norstrom, R.J., Mabury, S.A., Solomon, K., Evans, T.J., Stirling, I., Taylor, M.K., Muir, D.C.G., 2006. Temporal trends of perfluoroalkyl contaminants in polar bears (Ursus maritimus) from two locations in the North American Arctic, 1972–2002. Environ. Sci. Technol. 40, 1139–1143. https://doi.org/10.1021/es051750h.
Stock, N.L., Furdui, V.I., Muir, D.C.G., Mabury, S.A., 2007. Perfluoroalkyl contaminants in the Canadian Arctic: evidence of atmospheric transport and local contamination. Environ. Sci. Technol. 41, 3529–3536.
Thompson, W., 1994. Climate. Resource Description and Analysis: Ellesmere Island, National Park Reserve. 78. Parks Canada, National Resource Conservation Section, Prairie and Northern Region, Winnipeg, Canada.
USEPA, 2006. 2010/15 PFOA Stewardship Program. [WWW Document]. URL. https://www.epa.gov/assessing-and-managing-chemicals-under-tsca accessed 5.1.17.
Wang, S., Huang, J., Yang, Y., Hui, Y., Ge, Y., Larssen, T., Yu, G., Deng, S., Wang, B., Harman, C., 2013. First report of a Chinese PFOS alternative overlooked for 30 years: its toxicity, persistence, and presence in the environment. Environ. Sci. Technol. 47, 10163–10170. https://doi.org/10.1021/es401525n.
Wang, Z., Cousins, I.T., Scheringer, M., Buck, R.C., Hungerbuhler, K., 2014a. Global emission inventories for C4-C14 perfluoroalkyl carboxylic acid (PFCA) homologues from 1951 to 2030, part 2: the remaining pieces of the puzzle. Environ. Int. 69, 166–176.
Wang, Z., Cousins, I.T., Scheringer, M., Buck, R.C., Hungerbühler, K., 2014b. Global emission inventories for C4-C14 perfluoroalkyl carboxylic acid (PFCA) homologues from 1951 to 2030, part I: production and emissions from quantifiable sources. Environ. Int. 70, 62–75. https://doi.org/10.1016/j.envint.2014.04.013.
Wang, Z., Boucher, J.M., Scheringer, M., Cousins, I.T., Hungerbühler, K., 2017. Toward a comprehensive global emission inventory of C4-C10 perfluoroalkanesulfonic acids (PFSAs) and related precursors: focus on the life cycle of C8-based products and ongoing industrial transition. Environ. Sci. Technol. 51, 4482–4493. https://doi.org/10.1021/acs.est.6b06191.
Weber, A.K., Barber, L.B., Leblanc, D.R., Sunderland, E.M., Vecitis, C.D., 2017. Geochemical and hydrologic factors controlling subsurface transport of poly- and perfluoroalkyl substances, Cape Cod, Massachusetts. Environ. Sci. Technol. 51, 4269–4279. https://doi.org/10.1021/acs.est.6b05573.
Wong, F., Shoeib, M., Katsoyiannis, A., Eckhardt, S., Stohl, A., Bohlin-Nizzetto, P., Li, H., Fellin, P., Su, Y., Hung, H., 2018. Assessing temporal trends and source regions of per- and polyfluoroalkyl substances (PFASs) in air under the Arctic Monitoring and Assessment Programme (AMAP). Atmos. Environ. 172, 65–73. https://doi.org/10.1016/j.atmosenv.2017.10.028.
Yeung, L.W.Y., De Silva, A.O., Loi, E.I.H., Marvin, C.H., Taniyasu, S., Yamashita, N., Mabury, S.A., Muir, D.C.G., Lam, P.K.S., 2013. Perfluoroalkyl substances and extractable organic fluorine in surface sediments and cores from Lake Ontario. Environ. Int. 59, 389–397. https://doi.org/10.1016/j.envint.2013.06.026.
Yeung, L.W.Y., Dassuncao, C., Mabury, S., Sunderland, E.M., Zhang, X., Lohmann, R., 2017. Vertical profiles, sources, and transport of PFASs in the Arctic Ocean. Environ. Sci. Technol. 51, 6735–6744. https://doi.org/10.1021/acs.est.7b00788.
Young, C.J., Furdui, V.I., Franklin, J., Koerner, R.M., Muir, D.C.G., Mabury, S.A., 2007. Perfluorinated acids in Arctic snow: new evidence for atmospheric formation. Environ. Sci. Technol. 41, 3455–3461.
Zhu, Z., Wang, T., Wang, P., Lu, Y., Giesy, J.P., 2014. Perfluoroalkyl and polyfluoroalkyl substances in sediments from South Bohai coastal watersheds, China. Mar. Pollut. Bull. 85, 619–627. https://doi.org/10.1016/j.marpolbul.2013.12.042.
Zushi, Y., Tamada, M., Kanai, Y., Masunaga, S., 2010. Time trends of perfluorinated compounds from the sediment core of Tokyo Bay, Japan (1950s–2004). Environ. Pollut. 158, 756–763. https://doi.org/10.1016/j.envpol.2009.10.012.